Article

Influence of the Cable Accessories Installing Method on the Partial Discharge Activity in Medium Voltage Cables

Jacek Rybarz [1], Sebastian Borucki [1], Michał Kunicki [1,*], Aneta Kucińska-Landwójtowicz [2] and Dawid Wajnert [3]

[1] Department of Electrical Power Engineering and Renewable Energy, Opole University of Technology, 45-758 Opole, Poland; jacekrybarz@poczta.fm (J.R.); s.borucki@po.edu.pl (S.B.)

[2] Department of Management and Production Engineering, Opole University of Technology, 45-758 Opole, Poland; a.kucinska-landwojtowicz@po.edu.pl

[3] Department of Electrical Engineering and Mechatronics, Opole University of Technology, 45-758 Opole, Poland; d.wajnert@po.edu.pl

* Correspondence: m.kunicki@po.edu.pl

Abstract: This article proposes a method to modify the construction of a medium voltage (MV) heat shrinkable cable termination in cases of atypical damage to the shields of cross-linked polyethylene (XLPE) insulated cables. The proposed solutions include a modified method of assembling electric field control coating. An attempt was made to check the effect of such damage to the shields of MV cables with XLPE insulation on the level of occurrence of partial discharges within the cable termination. The investigations included testing the XRUHAKXS $1 \times 240/25$ cable type using the electric method (ME) and high frequency (HF) method with sinusoidal AC test voltage. As a result of the measurements, the values of total charges in the period and phase-resolved partial discharge (PRPD) patterns were obtained. The presented experimental results show the influence of the damage of the semiconducting coating surface on the occurrence of a defect in the cable termination without a modified method of control mantissa pinning. We suggest new methods of assembling MV cable accessories in the case of the presented coating damage in MV cable insulation.

Keywords: MV power cable; cable socket; cable head; partial discharge; electric field distribution control

1. Introduction

There is no doubt that medium voltage (MV) cable lines are a key element of the distribution network for distribution system operators (DSOs). Cable lines are usually used in stations where typical overhead lines cannot be applied (highly urbanized areas) or in case of the highest reliability requirements (plants or high priority customers). Currently built MV cable lines based on cross-linked polyethylene (XLPE) insulation replace older, much more unreliable cables, e.g., paper insulated lead covered (PILC) cables and those with polyethylene (PE) insulation [1,2].

The methods for assessing the technical condition of MV cable lines are usually based on statistical analyses of the failure events in a given section of the grid. This is an inaccurate method because it is based only on emergency events that have already taken place, and it involves only selected operational tests of a selected population of cable lines. For this reason, DSOs perform diagnostics of MV cable lines based mainly on partial discharge (PD) measurements and the dielectric loss factor ($tg\ \delta$) [3–5]. In case of cables in exploitation, the key objective of the PD tests is to identify and locate the source of PD [6–8]. However, diagnostic tests are also carried out on new and overhauled MV cables to confirm they meet the technical requirements prior to commissioning [9–11]. The most common failures in MV cables are directly related to cable equipment failures (Figure 1). This situation is mainly influenced by power grid anomalies (short circuits, overloads) and the associated thermal effects [12–16]. As a result, the highest possible quality and

durability of joints and cable terminations should be sought. The current development of technology and materials makes it possible to simplify the assembly process of cable equipment. Despite the efforts of manufacturers and electricians performing the installation work, the problem with exceeding the acceptable values of electric field strength (*E*) and the PD activity in the areas of terminations and joints still exists and plays a key role in the cable systems. A number of current studies are aimed at recognizing faults in XLPE cables and cable accessories [17–24]. Alternative methods have also been introduced for real-time monitoring of the cable systems using high frequency (HF) and ultra high frequency (UHF) methods [25–31].

Figure 1. Example of damage to a cable joint mounted on a cable type XRUHAKXS 1 × 240/50.

Analysis of the state of the art showed that not too many publications consider the unusual cases of semiconductor coating failure in the cable insulation system (Figure 2c), which may lead to failure of the entire cable insulation [15,27]. Therefore, the subject of this paper is to pay attention to the aspects of the correct method for installation of the cable terminations, which has a direct impact on the generation and development of PD in the MV cable lines. The results and analysis presented in the next part of this paper clearly show that the incorrect execution of a cable joint or cable termination directly affects the operation and reliability of the entire cable system. According to the authors' experience, some of the tools used in on-site work to remove the screen from the main insulation of the cable may significantly damage the insulation surface (Figure 2). A visual inspection of some newly assembled and finally unaccepted MV cable terminations (Figure 3) showed damage to the shield surface and deformation of the semiconductor coating. These are defects that in some perspective may lead to the PD. They are also very difficult to detect during the first on-site screening tests and even during typical commissioning tests after the assembly of the MV cable line [32–34].

Furthermore, this kind of fault is hard to fix without pre-preparing the cable for assembly, which requires cutting out another piece of the cable. It is not always possible in on-site scenarios because it involves pulling up the cable reserve, if there is any. The objective of this paper is to propose a modified method for minimizing the impact of imperfections (or even errors) during on-site cable equipment assembly work on the PD activity in MV cables. This method can be used in cases where the external semiconductor coating on the working insulation of the cable is damaged and when it is not possible to re-prepare the cable for the installation of cable accessories (e.g., no spare cable or it is not possible to pull it up, etc.). One of the prime assumptions for this method was to use only typical materials commonly available in the joints and terminations mounting kits in order to make it easy, inexpensive, and available for on-site applications. So far, none of the currently proposed methods has addressed (or solved) this problem. It is expected that this research would draw attention to the correct installation of the MV cable joints and connectors. Unfortunately, based on the authors' observations, these issues are often ignored in the construction of MV cable lines. Thus, this paper verifies the impact of the XLPE cable defect described above on the PD activity in the area of the MV cable terminal. Presented tests were conducted with particular consideration of the cable operation under real working conditions. The experimental studies clearly showed that the weakest elements of MV cable lines are their joints and terminations. Based on

laboratory tests, it has been shown that the elements with the lowest reliability in the cable line are its accessories, and the PD in MV cables usually occurs in incorrectly assembled joints and terminations. The presented method has already been implemented by DSOs with effective results.
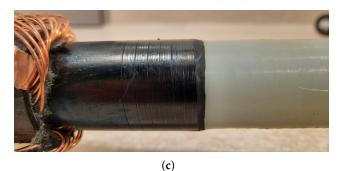

(**a**)   (**b**)

(**c**)

Figure 2. Process of preparing cable type XRUHAKXS 1 × 240/25 for installation of MV cable accessories: (**a**) device for removing shield from the insulation, (**b**) action removing shield from the cable insulation, (**c**) view of the cable shield after improper use of the device

(**a**)   (**b**)

Figure 3. MV separable tee shape connector: (**a**) external view, (**b**) view of shield damage and control mantis deformation

2. Materials and Methods

2.1. Heat Shrinkable Terminals of MV Cable

The test to determine the effect of the cable preparation quality for the cable termination assembly was carried out under laboratory conditions using heat-shrinkable MV cable

terminations. The prime assumption for this research was to use only typical materials commonly available in the joints and terminations mounting kits and used in on-site work for cables in exploitation. The cable terminations used in this research were 24-EPOT-1/70-240/(U) type, manufactured by Energy Partners, which are designed for connecting single-conductor cables with XLPE insulation and extruded screen at a rated voltage of 12/20 kV with MV distribution devices (switches, fuse bases) in overhead conditions. This type of termination can also be used in dusty and dirty environments (switching stations, transformer chambers) (Figure 4).
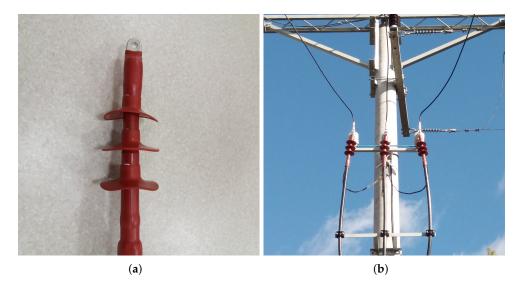

(**a**)   (**b**)

Figure 4. Heat shrinkable of MV cable termination type 24-EPOT-1/70-240/(U): (**a**) assembled cable head, (**b**) example of cable head application.

The termination structure includes conductive materials, insulating and controlling the electric field. The termination of the cable is a critical point due to the need to reduce the electric stresses caused by the change of the surface and shape of semi-conductive coatings, electric loads (thermal resistance of insulation), and protection against environmental conditions (moisture, significant differences in ambient temperature). For this reason, it is essential to select materials so that such phenomena occur at a minimum or not at all. Table 1 shows the components of the assembly kit.

Table 1. Elements of MV cable terminations type 24-EPOT-1/70-240/(U).

Item Number	Item Type	Elements View
1	Screw tip	
2	Heat-shrinkable cover CES-02	
3	Electrically insulating grease	
4	Insulating pipe RART 49/16-450	
5	RSCT 47/14-160 control tube	
6	EP MASTIK 30 mastic	
7	EP STRESS 20 control strap	

2.2. Research Model

The tests concerning the evaluation of the cable terminations installation method due to the generation of internal PD were carried out under laboratory conditions on the actual XRUHAKXS 1 × 240/25 cable model with a length of 5 m. According to the manufacturer's declaration and factory test protocols, the PD level did not exceed 2 pC. For experimental purposes, the construction of one of the terminations was modified.

Figure 5 shows a fragment of the assembly instructions for installing the EP-STRESS 20 control tape. According to Figure 5, one should tie the tape below 20 mm of the end of the screen, carefully fill the edge of the end of the screen on the insulation, and finish it with 10 mm on the insulation.
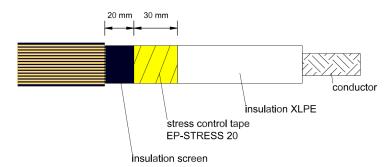
Figure 5. Correct assembly of the EP-STRESS 20 control strip according to the assembly instructions for the Energy Partners heat shrink termination type 24-EPOT-1/70-240/(U).

The modification introduced in this research consisted of adding an extra wrap of EP-STRESS 20 control tape over a larger area of the shield on one side of the cable (Figure 6b), which covered the damage to the shield caused by the stripping device. Further work on both terminations was carried out by the installation instructions. The modified termination was marked for later identification.
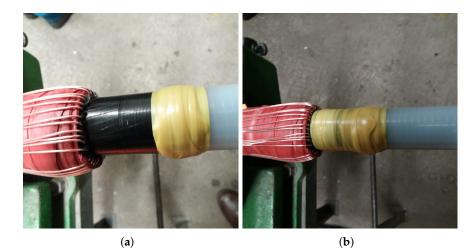
(**a**)   (**b**)

Figure 6. Stage of installation of the SN cable head type Energy Partners 24-EPOT-1/70-240/(U): (**a**) installation of the EP-STRESS tape on the cable surface according to the assembly instructions, (**b**) additional fastening of the tape on a larger area of the cable screen.

2.3. Measurement Methodology Adopted

The verification procedure included tests of the XRUHAKXS 1 × 240/25 cable with the simultaneous use of the ME and HF methods with the 50 Hz sinusoidal AC test voltage U_p, and a testing voltage ramp of 0 to 36 kV, which was three times the rated line voltage (new cables and equipment can be tested to this voltage). In actual field measurements, the tests should be performed up to twice the rated line voltage following IEC60502, IEEE

400.2. Due to the power limitations of test voltage sources for field tests caused by the cable line charging current, field test are performed using the very low frequency (VLF) methods or the wave oscillating test system (OWTS). The tests were performed in the following configurations:

1.　Cable type XRUHAKXS 1 × 240/25, 12/20 kV with ends of cable terminations type 24-EPOT-1/70-240/(U) with installed corona rings,
2.　Cable type XRUHAKXS 1 × 240/25, 12/20 kV with cable terminations type 24-EPOT-1/70-240/(U) without installed corona rings.

The purpose of the test without corona rings was to illustrate the operation of the cable line under actual conditions and to show the influence of the heterogeneity of the electric field distribution (*E*) at the screw terminals (Table 1, Item 1) on the appearance of PD in the cable termination area.

The test was carried out on a test bench equipped with the following devices (Figure 7):

1.　PS10-250 control panel,
2.　Capacitive voltage divider to measure the output voltage of the test transformer,
3.　TP test transformer with mains frequency $f = 50$ Hz and voltage ratio $\vartheta = 0.22/110 \left[\frac{kV}{kV}\right]$,
4.　Omicron MPD 600 PD analysis system, which includes:

　(a)　PC,
　(b)　MPD600 data acquisition unit,
　(c)　MCU504 control unit,
　(d)　CPL542 measuring impedance,
　(e)　CAL542 charge calibrator,
　(f)　MCC210 coupling capacitor,
　(g)　HFCT coil type 991/21.

To achieve the assumed research objective, several activities had to be carried out in order to determine the location of PD in the MV cable with cable terminations mounted. The experiment began with removing impurities and degreasing and dehumidifying the surfaces of the tested cables by washing them with isopropyl alcohol and technical acetone. The MV cable with the prepared cable terminations was placed on the test stand. One end of the cable equipped with the termination was connected to the output terminals of the test transformer, and the return conductors to the earthing busbar as shown in Figure 7. The other end of the cable was insulated from the ground potential with an MV strain relief isolator. The system was also calibrated using the CAL542 calibrator. The tests for each configuration began with increasing the test voltage to the value determined by the voltage ramp through automatic settings on the PS10-250 control panel. Measurement data were recorded with the Omicron MPD 600 system using two measurement tracks (ME and HF). The obtained measurement data were processed using the dedicated software.
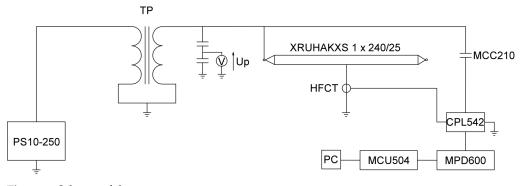

Figure 7. Scheme of the measurement system.

3. Results and Discussion

Results Analysis

As a result of the measurements carried out with the ME and HF methods, the values of apparent charge according to IEC60270 Q_{wtd}, maximum Q_{peak}, average Q_{avg} and PRPD measurement results were obtained. The results are presented in Tables 2–5 and Figures 8–11.

Table 2. Measurement results of Q depending on the U_p for the XRUHAKXS $1 \times 240/25$ cable with the corona rings installed.

Test Voltage	ME Method			HF Method		
	Q_{wtd} [1]	Q_{peak} [2]	Q_{avg} [3]	Q_{wtd} [1]	Q_{peak} [2]	Q_{avg} [3]
[kV]	[pC]	[pC]	[pC]	[pC]	[pC]	[pC]
12	14	22	14	10	27	10
17	16	22	15	13	24	12
20	16	19	16	13	17	12
22	15	21	16	13	23	13
26	30	125	16	25	115	13
32	145	270	130	142	249	123
36	115	250	129	119	229	122

[1] total charge per cycle IEC60270; [2] total charge per cycle max; [3] total charge per cycle average.
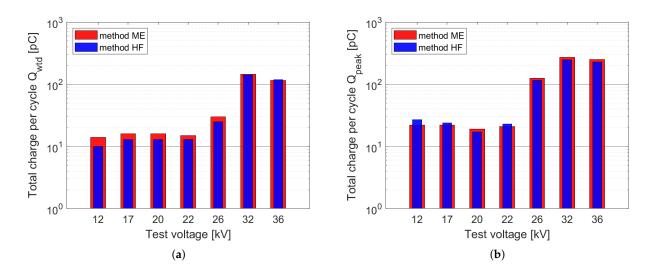
In the scenario with the corona rings, the value of the Q_{wtd}, under the influence of increasing the test voltage to the value of $U_p = 22$ kV, was practically constant at approximately 15 pC for the ME and HF methods. A slow increase to the value of approximately 30 pC occurred at the $U_p = 26$ kV. The subsequent increase of the voltage to $U_p = 32$ kV resulted in an increase of Q_{wtd} to the value of 145 pC and its decrease to 115 pC at the voltage of $U_p = 36$ kV.

The phenomenon of the decrease in the value of the Q on the surfaces of dielectrics and gas inclusions due to increasing the test voltage has been described in [35,36]. Possible causes of this phenomenon are an increase in the gas temperature and pressure caused by the development of PD and thus an increase in the conductivity of the insulation system in these areas, which leads to a decrease in the charge value. Such situations may occur, especially at the initial time of the performed tests.

For the Q_{peak} and Q_{avg} values, a similar situation occurred regarding their increase with the increase of the test voltage U_p. Furthermore, there was a decrease in the charge value for the U_p above 32 kV for both measurement methods. The analysis of PRPD images for the cable with installed corona rings for U_p range from 12 to 22 kV showed no PD increase in both half cycles, and their level was kept constant. The only noticeable value in this voltage range were single PD pulses that appeared at angles $\phi = 20°, 130°, 200°$, and $320°$. The intensity of these PD increased with increasing voltage values from 20 to 90 events per second.

In the case of U_p above 26 kV, in the negative part of the sinusoid between the angles $\phi = 180° \div 270°$, single PD pulses of low intensity (20 events per second) and values of approximately 100 pC were observed. Increasing the U_p to the value of 32 kV resulted in the appearance of a more significant number of PD of a similar intensity; their value increased to approximately 200 pC.

Additionally, PD appeared in the positive part of the sinusoid between the angles $\phi = 0° \div 90°$. The value of these PD was approximately 120 pC. With the test voltage $U_p = 36$ kV, the number and value of PD increased to 250 pC, and its level was higher in the negative half cycle of the supply voltage.
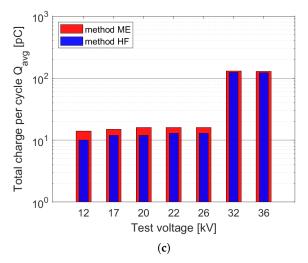
(**a**)

(**b**)

(**c**)

Figure 8. Values of apparent charge Q depending on the test voltage U_p for a cable with the installed corona rings registered with the ME and HF methods: (**a**) Q_{wtd}, (**b**) Q_{peak}, (**c**) Q_{avg}.
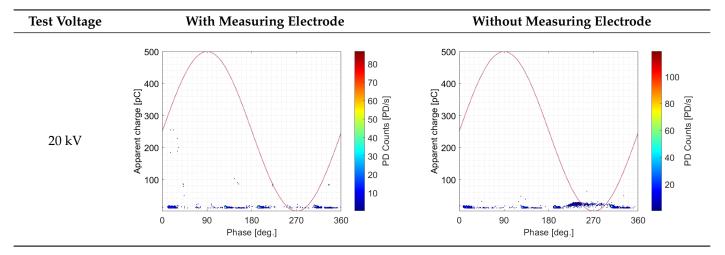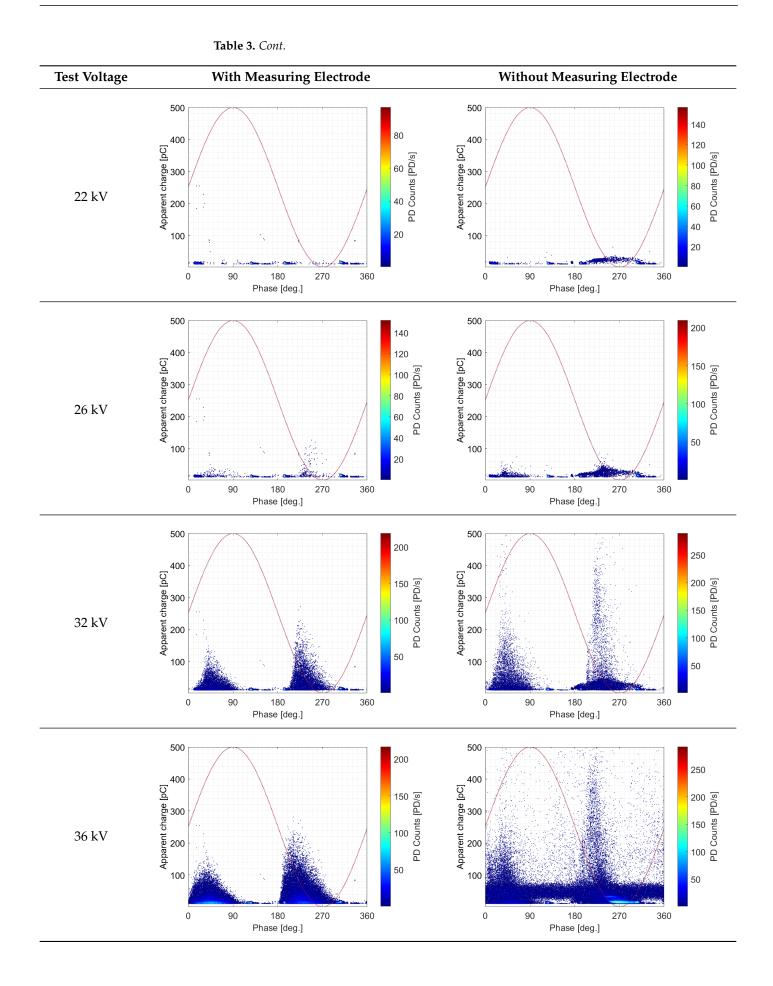
Table 3. PRPD images recorded by the ME method.

Test Voltage	With Measuring Electrode	Without Measuring Electrode
20 kV		

Table 3. *Cont.*

Test Voltage	With Measuring Electrode	Without Measuring Electrode
22 kV		
26 kV		
32 kV		
36 kV		

Table 4. Measurement results of Q depending on U_p for the XRUHAKXS $1 \times 240/25$ cable without installed corona rings.

Test Voltage	ME Method			HF Method		
	Q_{wtd} [1]	Q_{peak} [2]	Q_{avg} [3]	Q_{wtd} [1]	Q_{peak} [2]	Q_{avg} [3]
[kV]	[pC]	[pC]	[pC]	[pC]	[pC]	[pC]
12	14	48	14	11	53	10
17	20	27	16	20	25	13
20	23	63	21	25	66	21
22	30	36	24	30	39	25
26	48	82	33	41	74	35
32	537	989	353	514	1000	360
36	2707	136,700	8286	3831	112,400	8957

[1] total charge per cycle IEC60270; [2] total charge per cycle max; [3] total charge per cycle average.
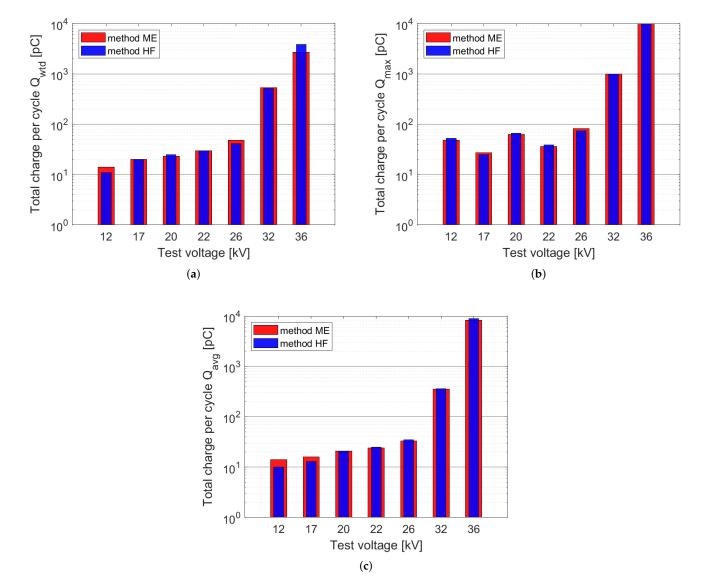

(**a**)

(**b**)

(**c**)

Figure 9. Graphical presentation of the value of Q depending on the U_p for a cable without installed corona rings, registered with the ME and HF method: (**a**) Q_{wtd}, (**b**) Q_{peak}, (**c**) Q_{avg}.
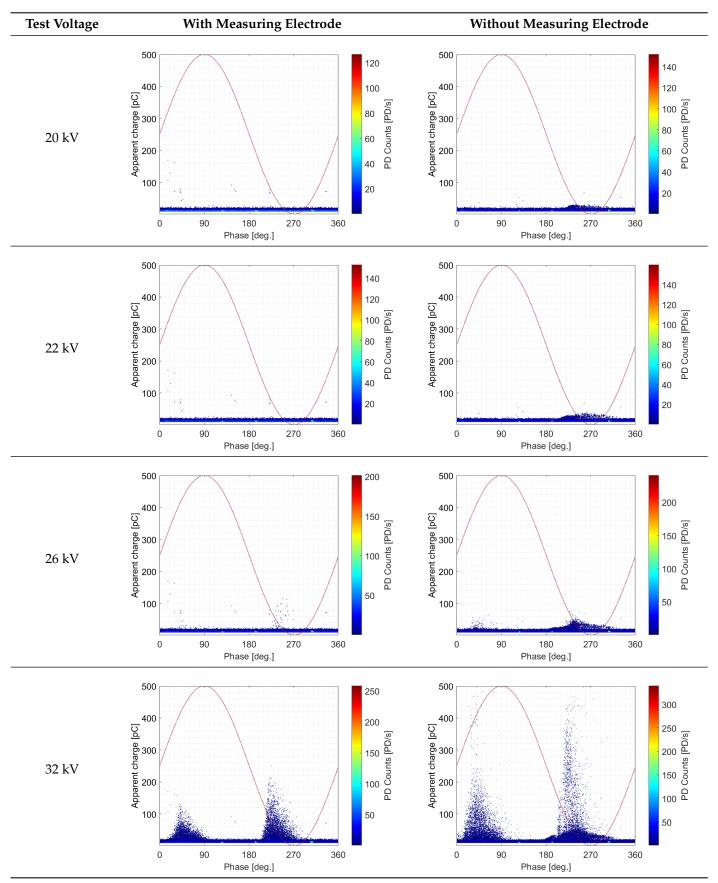
Table 5. PRPD images recorded with the HF method.

Test Voltage	With Measuring Electrode	Without Measuring Electrode
20 kV		
22 kV		
26 kV		
32 kV		

Table 5. *Cont.*

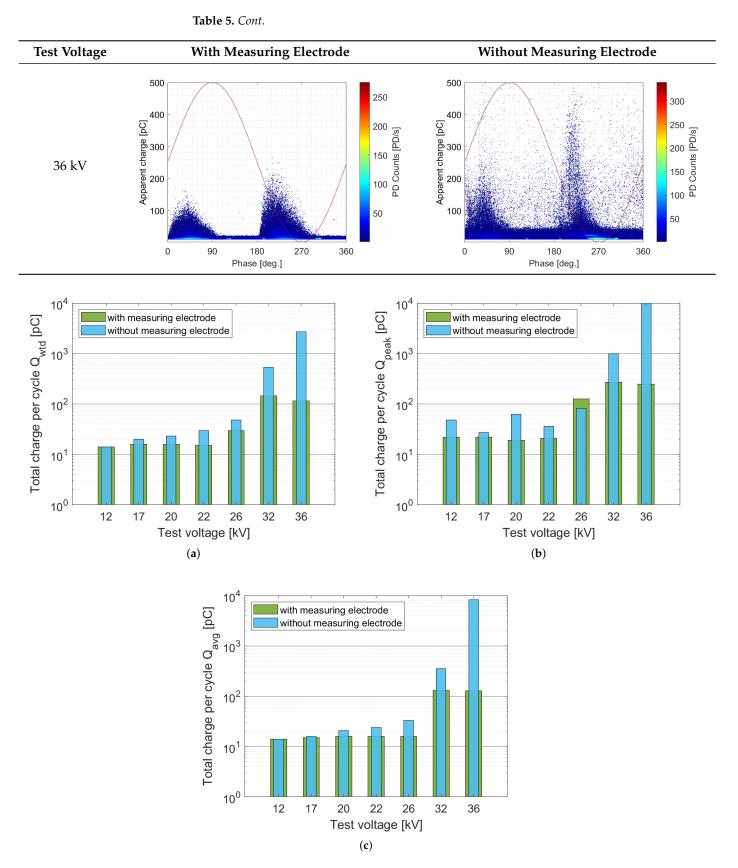| Test Voltage	With Measuring Electrode	Without Measuring Electrode
36 kV		

(**a**)

(**b**)

(**c**)

Figure 10. Graphical presentation of the value of Q depending on the U_p for a cable in a configuration with installed and removed corona rings using the ME method: (**a**) Q_{wtd}, (**b**) Q_{peak}, (**c**) Q_{avg}.

Another analysis involved the MV cable without corona rings on the cable terminations. The Q_{wtd} for the U_p in the range of 12 kV to 26 kV increased to the values of 48 pC and 41 pC for the ME and HF measurement methods. With the $U_p = 32$ kV, the Q_{wtd} value increased more than tenfold. In the case of the maximum and average charge values, such increases also occurred for both measurement methods. After removing the corona bells, an increased value of Q was noticed. This was due to the heterogeneity of the electric field strength on the uneven shapes of the cable terminal. An increase in U_p causes an increase in E in these places. An increase in Q in this situation was expected according to fundamental principles of the PD generation. After reaching the value of $U_p = 36$ kV, there was a defect and breakdown of the insulation in the cable terminations. The value of the registered Q_{max} reached the value of 136.7 nC for the ME method and 112.4 nC for the HF method, and the Q_{wtd} reached 2707 pC and 3831 pC, respectively. Figure 12 shows the successive stages of dismantling the insulation and control layers of the cable termination to confirm the location of the defect. The visible place (Figure 12d) with a diameter of approximately 4 mm and a depth of approximately 5 mm is damage to the surface of the cable insulation. The terminal of the semi-conductive coating and the insulation is at the contact point. It is a zone of discontinuity of the electric field. The surfaces of the EP-STRESS 20 control belt and the RSCT control tube were also damaged. This situation occured in the termination, which was mounted according to the assembly instructions. At the other end of the cable, where additional control tapes were attached to cover the entire surface of the semiconducting coating (Figure 6b), the cable was not damaged.
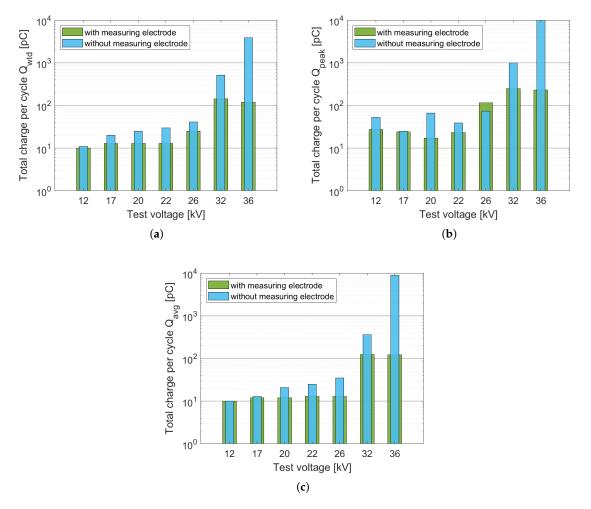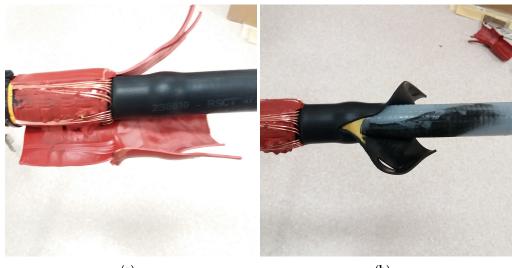

(a)

(b)

(c)

Figure 11. Graphical presentation of the value of Q depending on the U_p for a cable in a configuration with installed and removed corona rings using the HF method: (**a**) Q_{wtd}, (**b**) Q_{peak}, (**c**) Q_{avg}.

By analyzing the above event, the $Q(U_p)$ dependencies were determined for the ME and HF measurement methods, which are shown in Figure 13. The following dependencies show that the rapid increase in charge values occurred at the $U_p = 32$ kV (for both methods). Along with the further increase in the voltage value, the complete extinction of PD activity occurred (description of the phenomenon above). A very sharp increase in the value of Q, which exceeded 3 nC (ME method) and 4 nC (HF method), caused a cable insulation defect at the test voltage $U_p = 36$ kV. In practice, this situation indicates what Q value can cause immediate damage to the MV cable termination.

The analysis of PRPD images for the MV cable termination system without corona rings at $U_p = 12$ and 17 kV did not show an increase in PD for the ME and HF methods (only noise was recorded and single PD pulses). Forcing voltage from the value of $U_p = 20$ kV caused an increase in the number of PD with values not exceeding 50 pC with an intensity below 50 events/sec in the negative part of the sinusoid, in the phase range $\phi = 200° \div 330°$. With the $U_p = 32$ kV, the PD in both half-periods of the sine wave increased to maximum values of 500 pC. A characteristic form appeared in the range of phase angles ϕ 30° ÷ 60° and 210° ÷ 240° for both measurement methods (Tables 3 and 5).

This can probably be related to corona discharges on the copper ends of MV cable terminations. A very similar PD form was presented in [26], which represents the XLPE insulation with metal file inserts in a cable joint made on an MV cable with a voltage of 11 kV. Regarding the described sceanrio, it seems very likely that with this type of defect, the PD increase would be noticeable at the test voltage value below $U_p = 20$ kV. This form suggests an increase in PD in the insulation-metal connection in the tested MV cable termination.

The analysis of PRPD images at the test voltage $U_p = 36$ kV confirms the PD presence in the entire phase interval, which may be characteristic of the damage to the cable surface that occurred at this voltage.

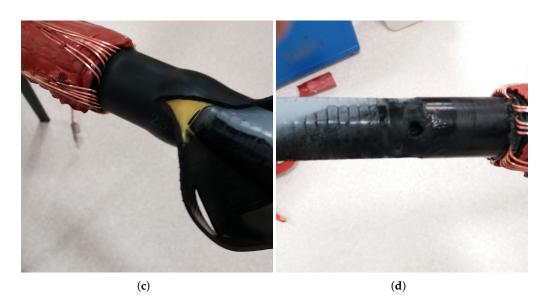(**a**)   (**b**)

Figure 12. *Cont.*

Figure 12. Damage to the surface of the insulation and the shield of the XRUHAKXS 1 × 240/25 cable at the MV cable termination: (**a**) disassembly of the insulating pipe RART 49/16-450, (**b**) disassembly of the control tube RSCT 47/14-160, (**c**) disassembly of the control strap EP STRESS 20, (**d**) view of damage to XLPE insulation
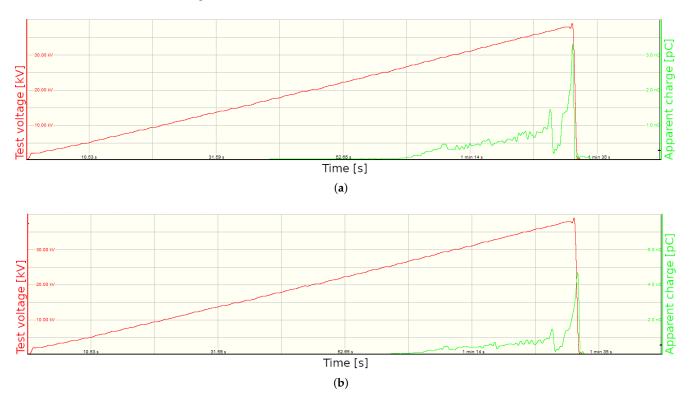

Figure 13. Waveforms of the $Q(U_p)$ dependence for the voltage ramp without corona rings: (**a**) ME method, (**b**) HF method.

4. Conclusions

The article proposes a method for modifying the structure of the MV heat-shrinkable cable termination in the event of damage to the shields of cables with XLPE insulation. The experimental results presented in Section 3 showed the effect of damage to the coating surface on the occurrence of a defect in the MV cable termination without a modified method of connecting the control tape. Correct assembly of all elements of the heat shrink

termination did not protect against insulation defects at test voltages above $U = 32$ kV. The presented test results are an attempt to indicate new, improved methods for mounting MV cable accessories in the case of the presented shield damages to the insulation of MV cables. However, it should be taken into account that the conducted experiment did not include a typical simulation of cable line operation under actual conditions (no-load, short line section). However, the tested object was also subjected to tests with a voltage higher than the rated voltage, making it challenging to interpret PD forms due to the appearance of charges on other surfaces that were not the subject of the study. The tests without the installed corona rings were aimed at bringing the experiment conditions closer to the on-site working conditions, in which the ends of the cable terminations are connected to the MV power grid apparatus. Their absence resulted in a double increase in the value of Q in the measurement system at a voltage of $U = 20$ kV upwards, which could have contributed to the damage to the cable termination in this experiment. An additional aspect worth emphasizing when testing cables with the presented defects is the phenomenon of the decrease in the value of Q in the system within a specific voltage range.

Conflicts of Interest: The authors declare no conflict of interest.

References

1. Hvidsten, S.; Holmgren, B.; Adeen, L.; Wetterstrom, J. Condition assessment of 12-and 24-kV XLPE cables installed during the 80s. Results from a joint Norwegian/Swedish research project. *IEEE Electr. Insul. Mag.* **2005**, *21*, 17–23. [CrossRef]
2. Gulski, E.; Smit, J.J.; Wester, F.J. PD knowledge rules for insulation condition assessment of distribution power cables. *IEEE Trans. Dielectr. Electr. Insul.* **2005**, *12*, 223–239. [CrossRef]
3. ElFaraskoury, A.; Mokhtar, M.; Mehanna, M.; Gouda, O. Conventional and un-conventional partial discharge detection methods in high voltage XLPE cable accessories. *Adv. Electr. Eng. Syst.* **2012**, *1*, 170–176.
4. Götz, D.; Petzold, F.; Putter, H.; Markalous, S.; Stephan, M. Localized PRPD pattern for defect recognition on MV and HV cables. In Proceedings of the 2016 IEEE/PES Transmission and Distribution Conference and Exposition (T&D), Dallas, TX, USA, 3–5 May 2016; pp. 1–4.
5. Álvarez Gómez, F.; Albarracín-Sánchez, R.; Garnacho Vecino, F.; Granizo Arrabé, R. Diagnosis of insulation condition of MV switchgears by application of different partial discharge measuring methods and sensors. *Sensors* **2018**, *18*, 720. [CrossRef]
6. Chang, W.; Gong, Y.; Bi, J.; Ma, G.; Zhuang, Y. High frequency partial discharge measurement of straight power cable joint. In Proceedings of the 2017 IEEE Electrical Insulation Conference (EIC), Baltimore, MD, USA, 11–14 June 2017; pp. 229–232.
7. Madonia, A.; Sanseverino, E.R.; Troia, I.; Bononi, S.F.; Giannini, S.; Mazzanti, G. Critical issues in the PD testing methodology for XLPE-insulated MV cables: an experimental case. In Proceedings of the 2017 IEEE Conference on Electrical Insulation and Dielectric Phenomenon (CEIDP), Fort Worth, TX, USA, 22–25 October 2017; pp. 311–314.
8. Wang, Y.; Wang, Y.; Wang, C.; Xu, H. The partial discharge characteristic of typical XLPE cable insulation defects under damped oscillating voltage. In Proceedings of the 2014 IEEE Electrical Insulation Conference (EIC), Philadelphia, PA, USA, 8–11 June 2014; pp. 290–293.
9. Hernandez-Mejia, J.C.; Harley, R.; Hampton, N.; Hartlein, R. Characterization of ageing for MV power cables using low frequency tan δ diagnostic measurements. *IEEE Trans. Dielectr. Electr. Insul.* **2009**, *16*, 862–870. [CrossRef]
10. Figueroa Godoy, F.; Jimenez, J.T.; Vacio, R.J.; Yáñez Mendiola, J.; Colin, J.Á. Analysis of Insulating Material of XLPE Cables considering Innovative Patterns of Partial Discharges. *Math. Probl. Eng.* **2017**, *2017*, 2379418. [CrossRef]

11. Mazzetti, C.; Mascioli, F.F.; Baldini, F.; Panella, M.; Risica, R.; Bartnikas, R. Partial discharge pattern recognition by neuro-fuzzy networks in heat-shrinkable joints and terminations of XLPE insulated distribution cables. *IEEE Trans. Power Deliv.* **2006**, *21*, 1035–1044. [CrossRef]

12. Bragatto, T.; Cerretti, A.; D'Orazio, L.; Gatta, F.M.; Geri, A.; Maccioni, M. Thermal Effects of Ground Faults on MV Joints and Cables. *Energies* **2019**, *12*, 3496. [CrossRef]

13. Bragatto, T.; Cresta, M.; Gatta, F.M.; Geri, A.; Maccioni, M.; Paulucci, M. Underground MV power cable joints: a nonlinear thermal circuit model and its experimental validation. *Electr. Power Syst. Res.* **2017**, *149*, 190–197. [CrossRef]

14. Ghaderi, A.; Mingotti, A.; Peretto, L.; Tinarelli, R. Effects of Temperature on MV Cable Joints Tan Delta Measurements. *IEEE Trans. Instrum. Meas.* **2019**, *68*, 3892–3898. [CrossRef]

15. Espín-Delgado, Á.; Letha, S.S.; Rönnberg, S.K.; Bollen, M.H.J. Failure of MV Cable Terminations Due to Supraharmonic Voltages: A Risk Indicator. *IEEE Open J. Ind. Appl.* **2020**, *1*, 42–51. [CrossRef]

16. Park, H.D.; Kim, J.S.; Jeong, I.B.; Choi, K.J.; Ryu, B.H.; Hong, J.W. Defect diagnosis of the cable insulating materials by partial discharge statistical analysis. In Proceedings of the 2009 IEEE 9th International Conference on the Properties and Applications of Dielectric Materials, Harbin, China, 19–23 July 2009; pp. 293–296.

17. Ahmed, Z.; Hussain, G.A.; Lehtonen, M.; Varacka, L.; Kudelcik, J. Analysis of partial discharge signals in medium voltage XLPE cables. In Proceedings of the 2016 IEEE 17th International Scientific Conference on Electric Power Engineering (EPE), Prague, Czech Republic, 16–18 May 2016; pp. 1–6.

18. Lee, J.S.; Koo, J.Y.; Lim, Y.S.; Kim, J.T.; Lee, S.K. An analysis of the partial discharge pattern related to the artificial defects introduced at the interface in XLPE cable joint using laboratory model. In Proceedings of the Annual Report Conference on Electrical Insulation and Dielectric Phenomena, Cancun, Mexico, 20–24 October 2002; pp. 482–485.

19. Jee Keen Raymond, W.; Illias, H.A.; Abu Bakar, A.H. Classification of partial discharge measured under different levels of noise contamination. *PLoS ONE* **2017**, *12*, e0170111. [CrossRef] [PubMed]

20. Montanari, G.C. Partial discharge detection in medium voltage and high voltage cables: Maximum distance for detection, length of cable, and some answers. *IEEE Electr. Insul. Mag.* **2016**, *32*, 41–46. [CrossRef]

21. Shafiq, M.; Kiitam, I.; Kauhaniemi, K.; Taklaja, P.; Kütt, L.; Palu, I. Performance comparison of PD data acquisition techniques for condition monitoring of medium voltage cables. *Energies* **2020**, *13*, 4272. [CrossRef]

22. Zhu, Z.; Huang, C.; Yu, Y.; Zhang, M.; Qin, Y. Research on partial discharge mechanism and characteristics for 10kV cable joint with air gap defect. In Proceedings of the 2014 China International Conference on Electricity Distribution (CICED), Shenzhen, China, 23–26 September 2014; pp. 1246–1250.

23. Ma, H.; Chan, J.C.; Saha, T.K.; Ekanayake, C. Pattern recognition techniques and their applications for automatic classification of artificial partial discharge sources. *IEEE Trans. Dielectr. Electr. Insul.* **2013**, *20*, 468–478. [CrossRef]

24. Jiang, Y.; Min, H.; Luo, J.; Li, Y.; Li, H.; Jiang, X.; Xia, R.; Li, W. Partial discharge pattern Characteristic of MV Cable joints with artificial defect. In Proceedings of the IEEE CICED 2010 Proceedings, Chengdu, China, 28–31 March 2010; pp. 1–3.

25. Singsathien, J.; Suwanasri, T.; Suwanasri, C.; Ruankon, S.; Fuangpian, P.; Namvong, W.; Saengsaikaew, P.; Khotsang, W. Partial discharge detection and localization of defected power cable using HFCT and UHF sensors. In Proceedings of the 2017 14th International Conference on Electrical Engineering/Electronics, Computer, Telecommunications and Information Technology (ECTI-CON), Phuket, Thailand, 27–30 June 2017; pp. 505–508.

26. Raymond, W.J.K.; Illias, H.A. High noise tolerance feature extraction for partial discharge classification in XLPE cable joints. *IEEE Trans. Dielectr. Electr. Insul.* **2017**, *24*, 66–74. [CrossRef]

27. Götz, D.; Putter, H.T. UHF pd-diagnosis at high voltage cable terminations—International case studies. In Proceedings of the 2017 IEEE INSUCON-13th International Electrical Insulation Conference (INSUCON), Birmingham, UK, 16–18 May 2017; pp. 1–5.

28. Abdullah, A.Z.; Rohani, M.N.K.H.; Isa, M.; Hamid, H.; Arshad, S.N.M.; Othman, M. Real On-Site Partial Discharge Measurement Technique in Medium Voltage Power Cable. In Proceedings of the 2018 IEEE 7th International Conference on Power and Energy (PECon), Kuala Lumpur, Malaysia, 3–4 December 2018; pp. 405–408.

29. Shafiq, M.; Kauhaniemi, K.; Robles, G.; Isa, M.; Kumpulainen, L. Online condition monitoring of MV cable feeders using Rogowski coil sensors for PD measurements. *Electr. Power Syst. Res.* **2019**, *167*, 150–162. [CrossRef]

30. Álvarez, F.; Garnacho, F.; Ortego, J.; Sánchez-Urán, M.Á. Application of HFCT and UHF sensors in on-line partial discharge measurements for insulation diagnosis of high voltage equipment. *Sensors* **2015**, *15*, 7360–7387. [CrossRef]

31. Milioudis, A.; Andreou, G.; Labridis, D. On-line partial discharge monitoring system for underground MV cables–Part II: Detection and location. *Int. J. Electr. Power Energy Syst.* **2019**, *109*, 395–402. [CrossRef]

32. Zhao, X.; Pu, L.; Ju, Z.; Ren, S.; Duan, W.; Wang, J. Partial discharge characteristics and development of typical XLPE power cable insulation defects. In Proceedings of the IEEE 2016 International Conference on Condition Monitoring and Diagnosis (CMD), Xi'an, China, 25–28 September 2016; pp. 623–626.

33. Wang, X.; Wang, C.C.; Wu, K.; Tu, D.M.; Liu, S.; Peng, J.K. An improved optimal design scheme for high voltage cable accessories. *IEEE Trans. Dielectr. Electr. Insul.* **2014**, *21*, 5–15. [CrossRef]

34. Metwally, I.A.; Al-Badi, A.H.; Al-Hinai, A.S.; Al Kamali, F.; Al-Ghaithi, H. Influence of design parameters and defects on electric field distributions inside MV cable joints. In Proceedings of the 2016 18th Mediterranean Electrotechnical Conference (MELECON), Lemesos, Cyprus, 18–20 April 2016; pp. 1–6.

35.   Wang, L.; Cavallini, A.; Montanari, G.C. Time behavior of gas pressure and PD activity in insulation cavities under AC voltage. In Proceedings of the 2010 Annual Report Conference on Electrical Insulation and Dielectic Phenomena, West Lafayette, IN, USA, 17–20 October 2010; pp. 1–4.

36.   Illias, H.; Chen, G.; Lewin, P.L. Partial discharge behavior within a spherical cavity in a solid dielectric material as a function of frequency and amplitude of the applied voltage. *IEEE Trans. Dielectr. Electr. Insul.* **2011**, *18*, 432–443. [CrossRef]